BIOCHEMISTRY
including biophysical chemistry & molecular biology

Article

pubs.acs.org/biochemistry

Identification and Characterization of a Tyramine–Glutamate Ligase (MfnD) Involved in Methanofuran Biosynthesis

Yu Wang, Huimin Xu, Kim C. Harich, and Robert H. White*

Department of Biochemistry, Virginia Polytechnic Institute and State University, Blacksburg, Virginia 24061, United States

Supporting Information

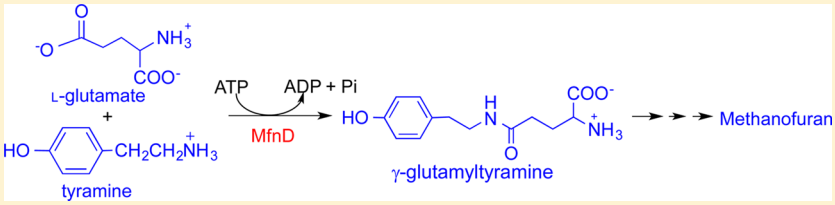

ABSTRACT: Methanofuran is the first in a series of coenzymes involved in the reduction of carbon dioxide to methane. All methanofuran structural variants contain a basic core structure of 4-[*N*-(γ-L-glutamyl-γ-L-glutamyl)-*p*-(β-aminoethyl)-phenoxymethyl]-2-(aminomethyl)furan (APMF-$(Glu)_2$) with different attached side chains depending on the source organism. Recently, we discovered the biosynthetic route for the production of 5-(aminomethyl)-3-furanmethanol-phosphate (F1-P), a precursor to the furan moiety of methanofuran. However, how the γ-linked glutamates are incorporated into methanofuran's structure remains unknown. Here, we report the identification of an ATP-grasp enzyme encoded by the gene Mefer_1180 in *Methanocaldococcus fervens* (the homologue of MJ0815 in *Methanocaldococcus jannaschii*, annotated as MfnD) that catalyzes the ATP-dependent addition of one glutamate to tyramine via a γ-linked amide bond. The occurrence of this reaction is consistent with the presence of γ-glutamyltyramine in cell extracts of *M. jannaschii*. Our steady-state kinetic analysis of the recombinant enzyme showed that MfnD exhibits a catalytic ability comparable to other ATP-grasp enzymes such as the *Escherichia coli* glutathione synthetase (GS), with a similar apparent k_{cat} and K_M. In addition, its activity is divalent metal-dependent, with the highest activity observed with Mn^{2+}. The previously solved crystal structure of MfnD from *Archaeoglobus fulgidus* exhibits a classical ATP-grasp fold with three structural domains; the ATP-binding and metal-binding motifs are conserved in MfnD as seen in other ATP-grasp enzymes. We used site-directed mutagenesis and kinetic analysis to demonstrate that Arg251 is an important residue for both catalysis and glutamate binding. By comparing the active site of MfnD with GS and by molecular docking substrates to the MfnD active site, we predicted the possible glutamate- and tyramine-binding pocket. This is the first report describing the enzymology of the incorporation of the initial L-glutamate molecule into the methanofuran structure. It also provides the first example of an ATP-grasp enzyme activating the γ-carboxylate of glutamate as substrate.

Methanofuran is the first coenzyme functioning in the reduction of carbon dioxide to methane during methanogenesis.[1−3] In addition, methylotrophic bacteria also use methanofuran as a coenzyme to oxidize formaldehyde to formic acid.[4,5] The chemical structure of methanofuran varies among different methanogens;[6] each methanofuran molecule contains the basic core structure of 4-[*N*-(γ-L-glutamyl-γ-L-glutamyl)-*p*-(β-aminoethyl)phenoxymethyl]-2-(aminomethyl)furan (APMF-$(Glu)_2$) but with different attached side chains. Recently, our laboratory identified a previously undescribed methanofuran in *Methanocaldococcus jannaschii*, which contains a long γ-glutamyl tail with 7−12 glutamates[57] (Figure 1). Although the function of methanofuran has been reported for many years, its biosynthetic pathway has not been fully elucidated.

Recently, we discovered the pathway to produce 4-(hydroxymethyl)-2-furancarboxaldehyde-P (4-HFC-P) from glyceraldehyde-3-P (Ga-3P)[a]. 4-HFC-P then undergoes a transamination reaction to produce 5-(aminomethyl)-3-furan-methanol-phosphate (F1-P),[7] a precursor to the furan moiety of methanofuran (Figure 1). We previously demonstrated that the MJ0050 gene encodes a tyrosine decarboxylase that produces tyramine from tyrosine.[8] However, the steps of how tyramine and glutamate are added to produce the final methanofuran product are still unknown. One of the steps in producing methanofuran requires a γ-linked amide bond formation between the tyramine moiety and the L-glutamate molecule.

Amide bond formation in living systems can usually be accomplished through either ribosomally mediated[9] or non-ribosomally mediated mechanisms.[10] The enzymes, which catalyze the formation of an amide bond, are known to produce a wide variety of natural products and coenzymes.[10−13] In addition to methanofuran, other coenzymes are known to contain amide bond(s) including F_{420}, coenzyme B, folate, B_{12}, and methanopterin.[14,15] Notably, in methanogens, both methanofuran and F_{420} contain γ-linked glutamates. During F_{420} biosynthesis, CofE in *M. jannaschii* catalyzes the GTP-

Received: July 17, 2014
Revised: September 10, 2014
Published: September 11, 2014

dx.doi.org/10.1021/bi500879h | *Biochemistry* 2014, 53, 6220−6230

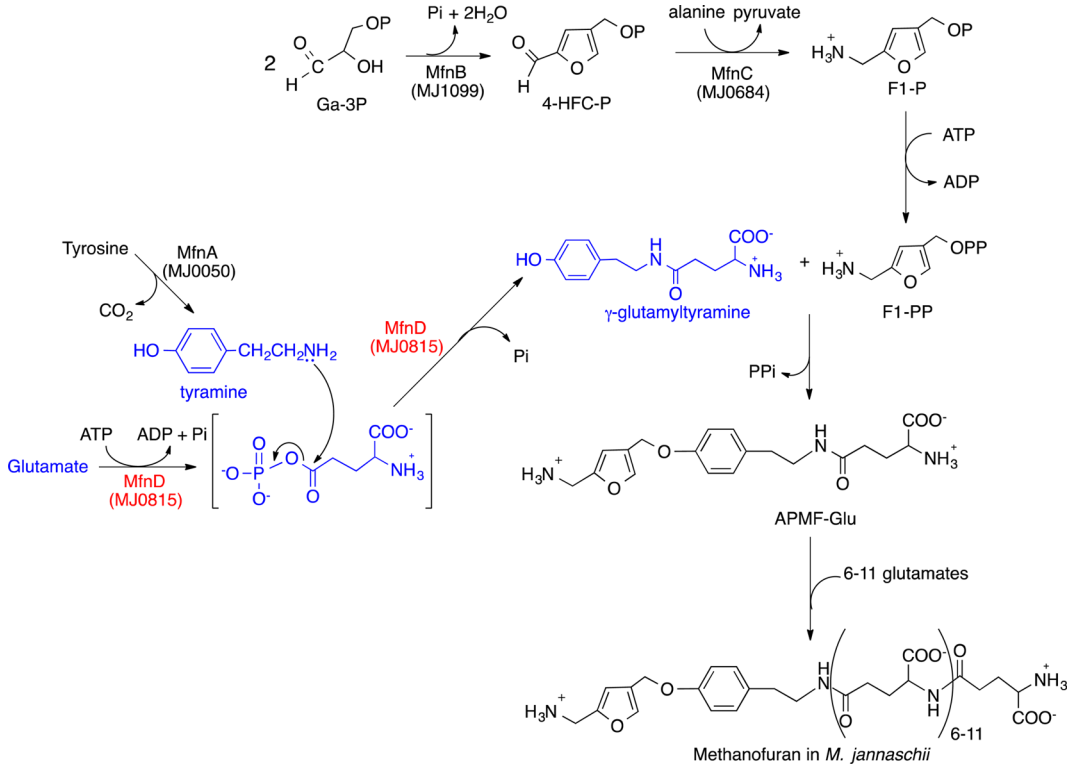

Figure 1. Biosynthetic pathway of methanofuran in *M. jannaschii*. Blue color represents the step and possible mechanism catalyzed by MfnD. Ga-3P, glyceraldehyde-3-P; F1-P, 5-(aminomethyl)-3-furanmethanol-phosphate; F1-PP, 5-(aminomethyl)-3-furanmethanol-pyrophosphate; 4-HFC-P, 4-(hydroxymethyl)-2-furancarboxaldehyde-phosphate; APMF, 4-[[4-(2-aminoethyl)phenoxy]-methyl]-2-furanmethanamine.

dependent addition of up to two γ-linked glutamates to F_{420}-0, producing F_{420}-2 in the presence of Mn^{2+}, Mg^{2+}, and K^+.[16] It is reasonable to assume that the two γ-linked glutamates could be added to methanofuran using the same strategy. However, the condensing group scenario is distinctive to methanofuran biosynthesis and is different from that observed in CofE. In the F_{420} biosynthesis pathway, the amine group of glutamate is coupled to an activated carboxylate group attached to the core structure,[16] whereas in methanofuran biosynthesis, the γ-carboxylate group of the first glutamate must be coupled to the amino group of the tyramine moiety. In this case, the glutamate must be activated at the γ-carboxylate group first, most likely by reacting with ATP to yield a reactive acyl phosphate intermediate, which could then undergo nucleophilic displacement of the phosphate by the amino group of the tyramine moiety. This strategy is seen within the ATP-grasp enzyme superfamily.[17,18]

ATP-grasp enzymes are described as a superfamily of enzymes with ATP-dependent carboxylate-amine or carboxylate-thiol ligase activities.[17,19,20] They share an atypical nucleotide-binding fold and two α + β domains that "grasp" a molecule of ATP between them.[18,21,22] In 2011, Fawaz et al. identified only 21 proteins as belonging to this superfamily.[18] Among these is the well-characterized glutathione synthetase (GS).[23,24] The complete genome sequence of the hyperthermophilic euryarchaeon *M. jannaschii* indicates that at least 12 gene products contain the ATP-grasp fold.[17,25] Ten of these have been assigned a specific function. These include the gene products of MJ0620 and MJ1001, which catalyze the addition of an α-linked L-glutamate to tetrahydromethanopterin and F_{420}-2 to form tetrahydrosarcinapterin and F_{420}-3, respectively.[26] At present, only the functions of MJ0776 and MJ0815 belonging to the ATP-grasp family are yet to be identified.[17] In addition, the homologue of MJ0815 (*orf1*) in *proteobacteria* and *planctomycetes*, present in a number of C_1 transfer gene clusters,[27] is believed to relate to formaldehyde oxidation/detoxification and methanopterin/methanofuran biosynthesis.[4,5,28] To test whether MJ0776 or MJ0815 catalyzes the formation of the amide bond between glutamate and the tyramine moiety, we have cloned and heterologously expressed both genes and their homologues (from *Methanocaldococcus fervens*) in *Escherichia coli*.

Here, we report that the purified protein expressed from the *M. fervens* gene locus Mefer_1180 (the homologue of MJ0815) catalyzes the ATP-dependent ligation of tyramine and glutamate to form γ-glutamyltyramine. This is the fourth enzyme that we have identified in the methanofuran biosynthetic pathway; therefore, we have annotated it as MfnD. In addition, we have characterized MfnD through a steady-state kinetic study and through site-directed mutagenesis. Our results suggest that Arg251 is important for both catalysis and glutamate binding. This is the first report of an enzyme responsible for adding a γ-linked glutamate to the tyramine moiety in the methanofuran structure. This work also establishes a new function for an ATP-grasp enzyme.

MATERIALS AND METHODS

Chemicals. All reagents were purchased from Sigma-Aldrich unless otherwise specified.

Synthesis of *N*-γ-Glutamyltyramine (2-Amino-5-((4-hydroxyphenethyl)amino)-5-oxopentanoic Acid). Tyramine (0.1 mmol, 13.6 mg) and *tert*-butyloxycarbonyl (BOC)-L-glutamate α-*tert*-butyl ester (0.1 mmol, 30.3 mg) were dissolved in 0.5 mL of tetrahydrofuran (THF) to produce a clear solution. Then, 0.12 mmol of dicyclohexylcarbodiimide

dx.doi.org/10.1021/bi500879h | *Biochemistry* 2014, 53, 6220−6230

(DCC) was added to the solution and the reaction incubated for 2 days at room temperature. The DCC-derived *N*,*N*′-dicyclohexylurea was then filtered from the reaction mixture. The desired product was isolated from filtrate by preparative thin layer chromatography (TLC), where it had an R_f = 0.23, using a solvent system consisting of acetonitrile, water, and 88% formic acid (19:2:1 vol/vol/vol). The final product showed the expected M^+ = 422 *m*/*z* in electron impact mass spectrometry, with a base peak at 120 and fragments at 107, 147, 221, 266, 293, and 322. This product was then deprotected by treatment with trifluoroacetic acid at room temperature for 30 min followed by evaporation of the solvent.

Synthesis of Furyltyramine (2-(4-(furan-3-ylmethoxy)-phenyl)ethan-1-amine). Because of the synthetic difficulties in preparing 4-[[4-(2-aminoethyl)phenoxy]-methyl]-2-furanmethanamine (APMF), we synthesized the structural analogue of APMF lacking the aminomethyl group to test as a substrate for MfnD. Tyramine (1 mmol, 137 mg) was placed in 2 mL of methylene chloride and 1 mL of water, followed by adding 1 mmol of sodium bicarbonate. To this well stirred sample, 1.1 mmol of di-*tert*-butyl dicarbonate (240 mg) in 1 mL of methylene chloride was added. After stirring for 30 min, the methylene chloride layer was removed and dried with sodium sulfate and then evaporated to give 248 mg of *tert*-butyl 4-hydroxyphenethylcarbamate (M^+ = 237 *m*/*z*). Furan-3-methanol (98 mg, 1.0 mmol) and triethylamine (188 μL, 1.35 mmol) were dissolved in 3 mL of THF and cooled to 0 °C, upon which 92 μL of mesyl chloride was slowly added with stirring. After 30 min, the sample was filtered to remove the precipitated triethylamine-HCl. The resulting clear solution was added at 0 °C to *tert*-butyl 4-hydroxyphenethylcarbamate dissolved in 3 mL of THF, to which 0.25 g of powdered sodium hydroxide and 52 mg of tetra-*n*-butylammonium bromide were added. The sample was stirred for 3 h at room temperature, filtered, and THF removed by evaporation using a stream of nitrogen gas. The residue was dissolved in 1 mL of methylene chloride that was washed with water and dried with sodium sulfate. Preparative TLC using 2.5% methyl acetate in methylene chloride as the solvent was used to purify the *tert*-butyl 4-(furan-3-ylmethoxy)phenethylcarbamate product (M^+ = 317 *m*/*z*). This sample was deprotected by treatment with an equal mixture of methylene chloride and trifluoroacetic acid for 1 min at room temperature and the solvent evaporated with a stream of nitrogen gas. LC-MS of the final product showed the expected MH^+ = 218 *m*/*z* with a strong fragment ion at 201 corresponding to $MH^+ - NH_3$. This analysis also demonstrated the presence of a small amount of tyramine (MH^+ = 138 *m*/*z*) produced during the deprotection step.

Isolation of γ-glutamyltyramine and γ-(glutamyl)$_2$tyramine from *M. jannaschii* Extracts. To a 100 μL sample of *M. jannaschii* cell extract prepared as previously described,[29] 16 μL of 6 M HCl was added and the precipitated proteins removed by centrifugation. The resulting clear aqueous layer was separated and heated at 100 °C for 5 min to release any F1 bound to methanofuran precursors.[3] The sample was centrifuged (16000*g*, 5 min) to remove the precipitated protein, and the supernatant was evaporated at room temperature with a stream of nitrogen gas. The resulting sample was dissolved in 50% methanol, and the contained γ-glutamyltyramine and γ-(glutamyl)$_2$tyramine were purified by preparative TLC. The resulting samples were analyzed by HPLC and LC-MS.

TLC Analysis and Purification of the Products. The TLC solvent used for the analysis and purification of amino acid adducts consisted of acetonitrile−water−formic acid (88%) (19:2:1 vol/vol/vol). In this solvent system, the following compounds had the following R_fs: tyramine, 0.50; α-glutamate, 0.125; γ-glutamyltyramine, 0.23; γ-(glutamyl)$_2$tyramine, 0.23. The tyramine and γ-glutamyltyramine were observed by UV absorption, and these compounds, as well as glutamate, were detected by ninhydrin spray.

LC-MS Analysis of the γ-Glutamyltyramine and Other Tyramine-Containing Compounds. Analysis was performed with an AB Sciex 3200 Q TRAP mass spectrometer system with an Agilent 1200 series liquid chromatograph. A Zorbax (100 mm × 4.0 mm, 2.6 μm particle size) column was used, and the injection volume was 15 μL. Solvent A was water with 25 mM ammonium acetate, and solvent B was methanol. The flow rate was 0.5 mL/min. Gradient elution was employed in the following manner (*t* (min), %B): (0.01, 5), (10, 65), (15, 65), (15.01, 5). Column effluent was passed through a variable wavelength detector set from 200−800 nm and then into the Turbo Spray ion source. Electrospray ionization (ESI) was employed at −4500 V and a temperature of 600 °C. Curtain gas, gas 1, and gas 2 flow pressures were 35, 70, and 60 psi, respectively. Desolvation, entrance, and collision cell entrance potentials were −40, −12, and −22.5 V, respectively.

HPLC Analysis of Tyramine and Tyramine Derivatives. Chromatographic separation and analysis of tyramine and tyramine derivatives were performed on a Shimadzu UFLC System equipped with a C_{18} reverse phase column (Varian Pursuit XRs 250 mm × 4.6 mm, 5 μm particle size), equipped with a photodiode array detector (PDA). The elution profile consisted of 5 min at 95% sodium acetate buffer (25 mM, pH 6.0, in the presence of 0.02% NaN_3) and 5% methanol followed by a linear gradient to 45% sodium acetate buffer/55% methanol over 40 min at 1.0 mL/min. Tyramine and γ-glutamyltyramine were detected by absorbance at 276 nm and confirmed by the full scan of UV spectrum. Under these conditions, ATP eluted at 3.0 min and ADP eluted at 3.6 min; tyramine and tyramine derivatives eluted in the following order (min): tyramine (10.6), γ-glutamyltyramine (17.8), and γ-aspartyltyramine (16.0).

Cloning of *M. jannaschii* MJ0815 and *M. fervens* Mefer_1180 Genes and Expression of their Gene Products. MJ0815 and its homologue Mefer_1180 were amplified from *M. jannaschii* and *M. fervens* genomic DNAs, respectively, by PCR. The primers used for MJ0815 were MJ0815-Fwd 5′-GGTGGTCATATGCTGTTACTCCAATC-3′ and MJ0815-Rev 5′-GATCGGATCCTTATTTGTC-TATTGTAAATTTTTC-3′. The primers used for Mefer_1180 were Mefer_1180-Fwd 5′-GGTCATATGATACTTTTCTTC-GAG-3′ and Mefer_1180-Rev 5′-GCTGGATCCTTATTTGT-TAATAGTAAATTC-3′. PCR amplifications were performed at 50 °C as the annealing temperature. The PCR products were purified, digested with *Nde*1 and *Bam*H1 restriction enzymes, and then ligated into compatible sites in plasmid pT7-7 to make the recombinant plasmid pMJ0815 and pMefer1180. The sequences were verified by sequencing at the University of Iowa DNA core facility. The resulting plasmids were used to transform the *E. coli* BL21-Codon Plus (DE3)-RIL (Stratagene). Transformed cells were grown in LB-medium (200 mL) supplemented with 100 μg/mL ampicillin at 37 °C with shaking until an OD_{600} of 1.0. Recombinant protein production was induced by addition of lactose to a final concentration of 28 mM. After an additional 4 h of culture at 37 °C, the cells were harvested by centrifugation (4000*g*, 5 min) and frozen at −20 °C. SDS-PAGE analysis of total cellular proteins confirmed the induction of MJ0815 and Mefer_1180 by the appearance of

intense protein bands at the expected 35 and 33 kDa molecular weight, respectively.

Generation of Mefer_1180 Mutants. The Quick-Change TM site-directed mutagenesis kit (Stratagene) was used to construct Mefer_1180 mutants according to manufacturer's instructions using template pMefer1180. Primers used for the mutants were Mefer1180-E21Q-Fwd 5′-GAAGGAATATTG-GAACAAGGAAAAATGATGTTTAAT AC-3′, Mefer1180-E21Q-Rev 5′-GTATTAAACATCATTTTTCCTTGTTCCAA-TATTCCTTC-3′, Mefer1180-R251A-Fwd 5′-CATTATAGA-GATTAATCCAGCAATTACAACAATC-3′, Mefer1180-R251A-Rev 5′-GATTGTTGTAATTGCTGGATTAATCTC-TATAATG-3′, Mefer1180-T253A-Fwd 5′-GAGATTAATC-CACGAATTGTAACAACAATCTATG-3′, and Mefer1180-T253A-Rev 5′-CATAGATTGTTGTTACAATTCGTGGATT AATCTC-3′. The sequences of plasmids carrying mutations were confirmed by sequencing (DNA Facility of Iowa University).

Purification of the Gene Products of Recombinant MJ0815, Mefer_1180, and Mefer_1180 Variants. A frozen *E. coli* cell pellet (~0.4 g wet weight from 200 mL of growth medium) was suspended in 3 mL of extraction buffer (50 mM TES, 10 mM $MgCl_2$, 20 mM DTT at pH 7.0) and lysed by sonication. The protein product from MJ0815 was expressed in inclusion bodies and not suitable for purification. In contrast, protein product from Mefer_1180, a homologue of MJ0815 (shares 76% sequence identity), was found to remain soluble even after heating to 80 °C. Therefore, the purification of the gene product of Mefer_1180 and its variants started with heating the resulting cell extracts for 10 min at 80 °C followed by centrifugation (16000*g*, 10 min). This process allowed the purification of the desired enzymes from the majority of *E. coli* proteins, which denature and precipitate under these conditions. Further purification was performed by anion-exchange chromatography of the 80 °C soluble fractions on a MonoQ HR column (1 cm × 8 cm; Amersham Bioscience) using a linear gradient from 0 to 1 M NaCl in 25 mM Tris buffer (pH 7.5), over 82 min at a flow rate of 1 mL/min. Fractions of 1 mL were collected. Protein concentrations were determined by Bradford analysis.[30]

Standard Enzymatic Assay of MfnD. The standard assay for measuring MfnD enzymatic activity was conducted in a 100 μL reaction volume containing 2 μg of wild-type MfnD, 5 mM tyramine, 5 mM L-glutamate, and 5 mM ATP in 50 mM TES buffer in the presence of 10 mM Mg^{2+} and 10 mM Mn^{2+} at pH 6.7 (pH measured at 70 °C) for 10 min at 70 °C. Following incubation, the reactions were quenched by the addition of 10 μL of 1 M TCA, the precipitated protein was removed by centrifugation (16000*g*, 10 min), and the resulting sample was neutralized by adding 8.3 μL of 1.5 M, pH 8.8, Tris buffer. The samples were analyzed by HPLC.

Establishing the Nature of the Amide Bond Formed by MfnD. The nature of the amide bond linkage between tyramine and glutamate was determined by incubation of the reaction product with peptidases of known specificity. The peptidases used were carboxypeptidase Y (specifically removes carboxyl terminal α-amino acid) and γ-glutamyl transpeptidase (specifically transfers the terminal γ-glutamyl group to an acceptor molecule such as glycylglycine). After completing the MfnD standard assay reaction, 50 μL of each reaction mixture was treated with no peptidase, 5 μL of carboxypeptidase Y (0.16 U/μL), or 5 μL of γ-glutamyl transpeptidase (0.5 U/μL in the presence of 100 mM glycylglycine), respectively, in 100 mM Tris buffer, pH 8.0, at room temperature for 2 h. The products were then analyzed by HPLC.

The pH and Metal-Dependence of the MfnD Catalyzed Reaction. To investigate the influence of pH on catalytic ability, the specific activity at varying pH was measured. The standard enzymatic assays were conducted in 25 mM Tricine/CAPS/TES buffer from pH 5.9 to 10.5 (pH measured at 70 °C) for 10 min at 70 °C. For the metal-dependent study, the standard enzymatic assays were carried out including 10 mM of one of the following cations: Mg^{2+}, Mn^{2+}, Ni^{2+}, Co^{2+}, Cu^{2+}, Zn^{2+}, or K^+, replacing Mg^{2+} and Mn^{2+} in the standard assay.

Substrate Specificity. Substrate specificity of MfnD was investigated using different nucleotides and amino acids. Under the standard enzymatic assay condition, specific activities were measured using 5 mM UTP, CTP, or GTP instead of ATP. In addition, 5 mM L-pyroglutamate, *N*-acetyl-L-glutamate, L-aspartate, L-α-aminoadipic acid, γ-glutamylglutamate instead of L-glutamate, and 5 mM L-tyrosine, L-phenylalanine, L-phenylethylamine, and furyltyramine (~1 mM) instead of tyramine were used to evaluate the substrate specificity of MfnD.

Steady-State Kinetic Study. The apparent kinetic parameters were determined by measuring γ-glutamyltyramine formation catalyzed by MfnD in a 100 μL reaction volume. For the tyramine-dependent kinetic study, the reaction included one of the following enzymes with the indicated amounts (2 μg of wild-type, 4 μg of E21Q, 4 μg of T253A, or 10 μg of R251A), 10 mM ATP, and 50 mM L-glutamate incubated with varying concentrations of tyramine (0.05−10 mM) in 50 mM TES buffer, pH 6.7 (pH measured at 70 °C), in the presence of 10 mM Mg^{2+} and Mn^{2+} for 10 min (50 min for R251A) at 70 °C. For the glutamate-dependent kinetic study, the reaction was conducted in the same buffer and conditions including an enzyme (see above), 10 mM tyramine, and 10 mM ATP incubated with varying concentrations of glutamates (0.05−50 mM). For the ATP-dependent kinetic study, an enzyme (see above) was incubated with 10 mM tyramine, 50 mM glutamate, and varying ATP concentrations (0.01−10 mM) in the same buffer and conditions. Following incubation, the reactions were quenched by the addition of 10 μL of 1 M TCA, the protein precipitate was removed by centrifugation (16000*g*, 10 min), and the resulting supernatant was neutralized by adding 8.3 μL of 1.5 M pH 8.8 Tris buffer. The resulting samples were then analyzed by HPLC. The apparent kinetic constants were calculated by fitting the data to the Michaelis−Menten equation using prism 5.0c.

Molecular Docking of Glutamate and Tyramine into MfnD. The L-glutamate and tyramine structures were obtained from the RCSB Protein Data Bank (PDB 4IWX and PDB 3BRA, respectively). The X-ray crystal structure data of MfnD from *Archaeoglobus fulgidus* was deposited in the Protein Data Bank as PDB 3DF7. The protein and substrate files for molecular docking were prepared using AutoDock Tools 1.5.6.[31] Each substrate was docked to the MfnD active site separately. AutoDock Vina[32] built in Chimera[33] was used to perform the molecular docking of L-glutamate and tyramine into MfnD. The parameters of molecular docking for L-glutamate were a box size of 32 Å × 2 Å × 5 Å that was centered within the coordinates (40, 48, 35). The parameters of molecular docking for tyramine were a box size of 20 Å × 10 Å × 8 Å that was centered within the coordinates (15, 15, 15). The models we chose considered both energy and reasonable orientation and conformation.

dx.doi.org/10.1021/bi500879h | *Biochemistry* 2014, 53, 6220−6230

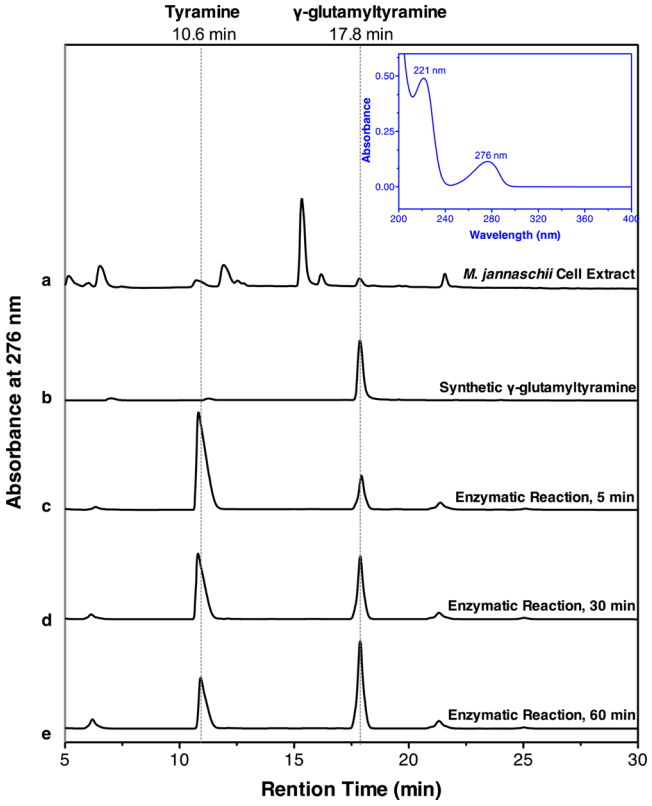

Figure 2. HPLC analysis of the TLC purified *M. jannaschii* cell extract fraction (a), the synthetic γ-glutamyltyramine (b), the MfnD catalyzed reaction incubated at 70 °C for 5 min (c), 30 min (d), and 60 min (e). Inset: UV−vis absorption spectrum of the known γ-glutamyltyramine (synthetic γ-glutamyltyramine), which was eluted at 17.8 min from an HPLC C_{18} reverse phase column showing absorbance maxima at 221 and 276 nm.

RESULTS AND DISCUSSION

Characterization of Synthetic γ-Glutamyltyramine. The synthetic γ-glutamyltyramine showed a single HPLC peak eluting at 17.8 min with absorbance maxima at 221 and 276 nm (Figure 2b,inset). Tyramine had the same absorbance maxima and eluted at 10.6 min. LC-MS showed a single peak with $MH^+ = 267.13$ m/z and $(M - H)^- = 265.12$ m/z. MS/MS of the $MH^+ = 267.13$ m/z ion showed fragments at 250, 221, 204, 138, 130, 121, 103, 93, 91, and 84. MS/MS of the $(M - H)^- = 265.12$ ion showed fragments at 247, 221, 219, 190, 127, 119, and 109.

Table 1. Apparent Steady-State Kinetic Parameters of MfnD and Its Variants

	wild-type	E21Q	R251A	T253V
Tyramine-Dependent Apparent Kinetic Parameters[a]				
$k_{cat(app)}$ (s^{-1})	4.8 ± 0.2	1.7 ± 0.1	0.05 ± 0.01	1.4 ± 0.1
$K_{M(app)}$ (mM)	0.80 ± 0.1	1.1 ± 0.2	0.80 ± 0.3	0.60 ± 0.2
$k_{cat(app)}/K_{M(app)}$ (M^{-1} s^{-1})	6.0×10^3	1.7×10^3	6.0×10^1	2.3×10^3
Glutamate-Dependent Apparent Kinetic Parameters[b]				
$k_{cat(app)}$ (s^{-1})	5.8 ± 0.7	2.7 ± 0.5		1.3 ± 0.1
$K_{M(app)}$ (mM)	2.3 ± 0.8	7.3 ± 2	≥40	3.6 ± 0.6
$k_{cat(app)}/K_{M(app)}$ (M^{-1} s^{-1})	2.5×10^3	3.7×10^2		3.6×10^2
ATP-Dependent Apparent Kinetic Parameters[c]				
$k_{cat(app)}$ (s^{-1})	5.9 ± 0.3	2.1 ± 0.1	0.07 ± 0.01	1.4 ± 0.1
$K_{M(app)}$ (mM)	1.5 ± 0.2	2.0 ± 0.3	3.0 ± 1.0	2.5 ± 0.5
$k_{cat(app)}/K_{M(app)}$ (M^{-1} s^{-1})	3.9×10^3	1.1×10^3	2.3×10^1	5.6×10^2

[a]The reaction included one of the enzymes in the following amounts (2 μg of wild-type, or 4 μg of E21Q or 4 μg of T253A or 10 μg R251A), 10 mM ATP, and 50 mM L-glutamate incubating with varying concentrations of tyramine (0.05−10 mM) in 50 mM TES buffer, pH 6.7 (pH measured at 70 °C), in the presence of 10 mM Mg^{2+} and Mn^{2+} for 10 min (50 min for R251A) at 70 °C. [b]The reaction was conducted in the same buffer and conditions including an enzyme (see above), 10 mM tyramine, and 10 mM ATP, incubated with varying concentrations of glutamate (0.05−50 mM). [c]An enzyme (see above), was incubated with 10 mM tyramine, 50 mM glutamate, and varying concentrations of ATP (0.01−10 mM) in the same buffer and conditions.

Identification of γ-Glutamyltyramine and γ-(Glutamyl)$_2$-tyramine in *M. jannaschii* Cell Extracts. The existence of γ-glutamyltyramine from *M. jannaschii* cell extracts was confirmed by high resolution mass spectral analysis (Supporting Information Figure 1A) and HPLC (Figure 2a); the existence of γ-(glutamyl)$_2$tyramine was inferred from high resolution mass spectral data by a single peak $(M - H)^- = 394.16$ m/z and $MH^+ = 396.18$ m/z (Supporting Information Figure 1B). The amount of γ-(glutamyl)$_2$tyramine was less than 5% of the γ-glutamyltyramine in the *M. jannaschii* cell extracts based on the total ion intensity from the data obtained in both negative and positive ion mode. This indicated that γ-glutamyltyramine was likely an intermediate in methanofuran biosynthesis. The condensation of γ-glutamyltyramine with 5-(aminomethyl)-3-furanmethanol-py-

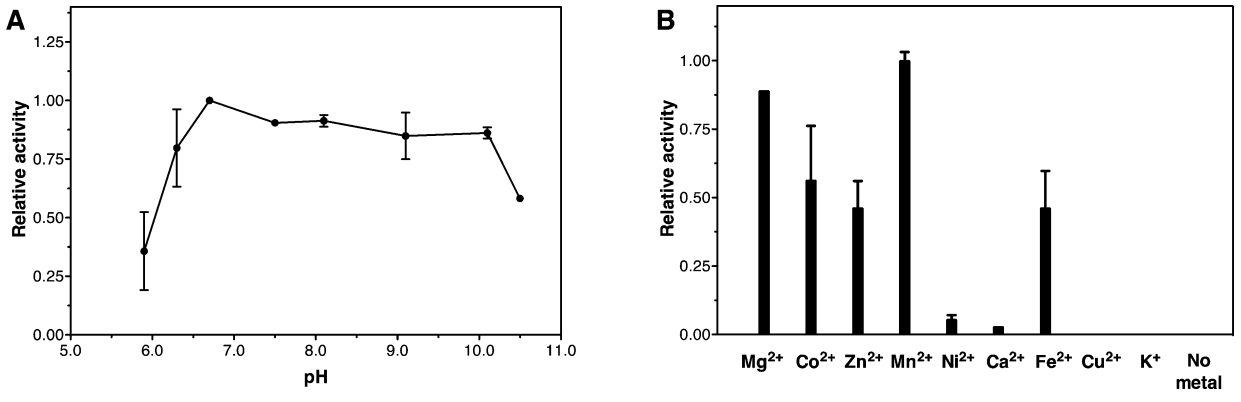

Figure 3. (A) The pH profile of MfnD. (B) The metal-dependent study of MfnD.

dx.doi.org/10.1021/bi500879h | *Biochemistry* 2014, 53, 6220−6230

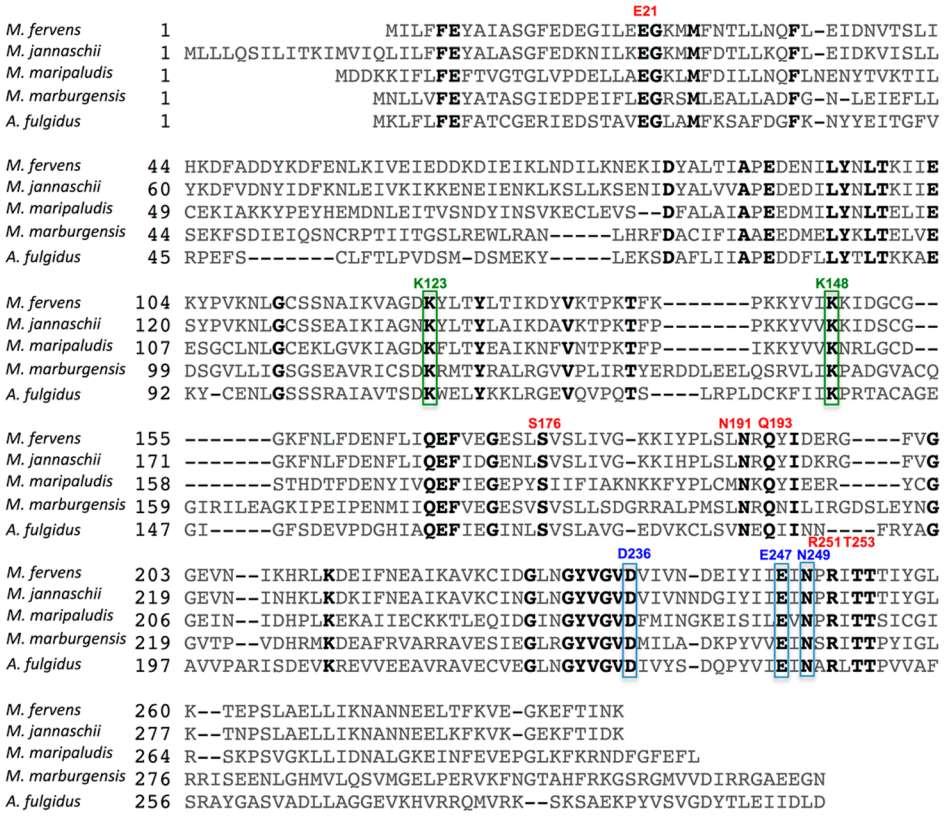

Figure 4. Multiple sequence alignment of MfnD homologues. Green boxes highlight residues interacting with ATP/ADP molecules in the active site. Blue boxes highlight residues interacting with metal ions. Multiple sequence alignment was conducted presented using Alignment-Annotator web server.[55] The accession numbers of each sequence are as follows: *M. fervens*, C7P8V7; *M. jannaschii*, Q58225; *Methanococcus maripaludis*, A4FYR4; *Methanothermobacter marburgensis*, D9PX73; *A. fulgidus*, O29201.

rophosphate (F1-PP) likely occurs after γ-glutamyltyramine formed (Figure 1), unlike folate biosynthesis where the first glutamate molecule is added only after dihydropteroate is formed.[34,35] In addition, no more than two glutamates linked to a tyramine molecule was found in the cell extract.

Recombinant Expression, Purification, and Analysis of the Gene Products of MJ0815, Mefer_1180, and Mefer_1180 Variants. The gene product of MJ0815 was expressed in inclusion bodies. Therefore, its homologue from *M. fervens* (Mefer_1180) was cloned and overexpressed in *E. coli*. Its gene product (Supporting Information Figure 2) and its three substitution variants were found to remain soluble and were purified by heating the cell extract to 80 °C followed by anion exchange chromatography. The purified protein migrated as a single band and was greater than 90% pure with an apparent molecular mass of 33 kDa as evaluated by SDS-PAGE. The identity of the purified protein (wild-type Mefer_1180) was also confirmed by MALDI-MS of the tryptic-digested protein band from the SDS gel (Supporting Information Table 1).

The Gene Product of Mefer_1180 Is a Tyramine–Glutamate Ligase (MfnD). The homologues of MfnD are widely distributed among the methanofuran-containing organisms, including all methanogenic archaea and some methylotrophic bacteria, consistent with its essential role in methanofuran biosynthesis. Incubation of MfnD with the possible substrates, tyramine or furyltyramine with L-glutamate in the presence of ATP, clearly showed that MfnD catalyzed the formation of the amide bond between tyramine and glutamate. The ATP molecule was hydrolyzed to ADP, which was confirmed by coelution with a known ADP standard by HPLC (data not shown). A control experiment containing the same concentration of substrates in the absence of MfnD showed none of the expected product. The resulting product from the reaction catalyzed by MfnD was observed as a single HPLC peak eluting at 17.8 min with absorbance maxima at 221 and 276 nm (Figure 2c–e), consistent with the synthetic γ-glutamyltyramine (Figure 2b). The amount of product from the enzymatic reaction increased with incubation time (Figure 2c–e) and could be digested by γ-glutamyl transpeptidase (in the presence of glycylglycine) but not by carboxypeptidase Y (which specifically digests the α-linked amide bonds), further indicating the amide bond between tyramine and glutamate was γ-linked. In addition, MfnD cannot use furyltyramine as a substrate, which was inferred from LC-MS data (data not shown). This is consistent with the observation that γ-glutamyltyramine is the enzymatic product of MfnD and its presence in *M. jannaschii* cell extracts. It also suggested the condensation of the tyramine moiety with F1-PP would most likely occur after formation of γ-glutamyltyramine. This is in contrast to F_{420} biosynthesis, where CofE catalyzes the GTP-dependent addition of two L-glutamates on the L-lactyl phosphodiester of F_{420}-0 to form F_{420}-2.[16] MfnD almost exclusively catalyzed the ATP-dependent addition of one L-glutamate to tyramine. Only when more than 10 μg of MfnD was added to the standard reaction was a trace of γ-(glutamyl)$_2$tyramine (the intensity was less than 2% of γ-glutamyltyramine) detected by LC-MS in the negative ion mode. The ratio of γ-glutamyltyramine and γ-(glutamyl)$_2$tyramine did not change by extending the incubation time.

Enzymatic and Physical Properties of MfnD. Wild-type MfnD and its three variants were all found to possess high

dx.doi.org/10.1021/bi500879h | *Biochemistry* 2014, 53, 6220–6230

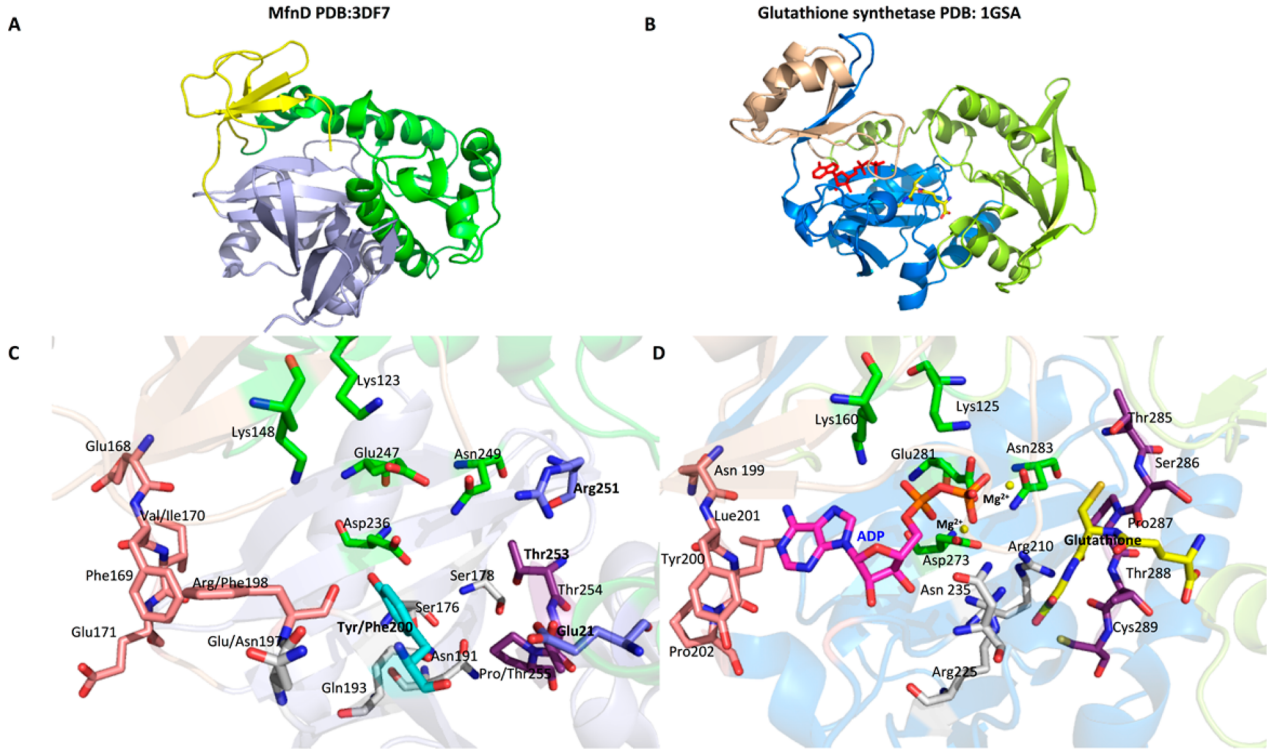

Figure 5. Comparison of the monomer structure of MfnD (left, PDB 3DF7) and GS (right, PDB 1GSA) (A,B); comparison of the active site of MfnD and GS (C,D). Numbering of MfnD reflects the gene product of Mefer_1180 and numbering of GS reflects *E. coli* GS. The bound molecules in GS highlighted by pink and yellow represent ADP and glutathione molecules, respectively. Yellow spheres represent the bound Mg^{2+}. Figure is generated and presented using MacPyMOL 1.3.[56]

thermal stability following heating at 80 °C for 30 min. Moreover, they all exhibit high stability at high pH because no protein aggregation and precipitation was observed when proteins were incubated for 10 min at 80 °C in 25 mM Tricine/CAPS/TES buffer at pH 10.5. The pH-dependent study showed a very broad pH optimum with a maximum around pH 6.7. More than 50% of the activity was still observed when the reaction was carried out at pH 10.5 (Figure 3A).

For the ATP-grasp enzymes, usually one to three Mg^{2+} ions interact with the phosphate moiety of the bound ATP,[18] with the exception of synapsin Ia, in which one Ca^{2+} is found in the active site.[22,36,37] Therefore, the cation requirement of MfnD was examined by assaying in the presence of different cations (Figure 3B). No activity was detected in a reaction that lacked added metals. Maximum activity (100%) was observed with the addition of 10 mM Mn^{2+}, followed by 89%, 56%, 46%, and 46% of relative activity by addition of 10 mM Mg^{2+}, Co^{2+}, Zn^{2+}, and Fe^{2+}, respectively. Less than 5% relative activities were observed when 10 mM Ni^{2+} or Ca^{2+} was added. However, no activity was detected by addition of Cu^{2+} or K^{+}. Although most ATP-grasp enzymes have Mg^{2+} ions interacting with the phosphate groups of ATP, Mn^{2+} substituting for Mg^{2+} as Lewis acid (in this case, facilitating the phosphate transfer) is often observed.[38] Our results showed that MfnD could employ a wide range of divalent metal ions, however, some divalent metal ions and monovalent metal ions exhibited no or poor ability to activate the activity of MfnD. A possible explanation is that some divalent metal ions such as Ca^{2+} and Cu^{2+} could not form an outer-sphere complex (interaction with a water molecule between the metal ion and N7 of ATP molecule), which represents the steric requirement for the ATP−metal complex at the active site.[39] Furthermore, a similar profile of metal dependence has also been observed in other ATP-grasp enzymes such as GS[40] and 5-formaminoimidazole-4-carboxamide-1-β-D-ribofuranosyl 5′-monophosphate synthetase (*PurP*).[41]

Substrate Specificity. The effectiveness of various nucleotides as substrates for MfnD was tested. As expected, MfnD exhibited maximum activity with ATP (100%). Activities with UTP (<0.2%), CTP (<0.08%), and GTP (<0.04%) were much lower. Reactions using tyrosine or phenylalanine instead of tyramine showed none of the expected products. Interestingly, phenylethylamine could also be used as substrate to form the γ-glutamylphenylethylamine as shown by a single peak with MH^{+} = 251.2 m/z and $(M - H)^{-}$ = 249.1 m/z from LC-MS. However, free phenylethylamine was never observed in *M. jannaschii* cell extracts. In contrast, MS analysis of the amino acid fraction of cell extracts from five different methanogens as well as *A. fulgidus* all demonstrated the presence of free tyramine (Supporting Information). This indicated that the natural substrate of MfnD was tyramine and not phenylethylamine, although MfnD apparently could not differentiate phenyethylamine and tyramine. LC-MS and HPLC analyses of enzymatic assays including L-aspartate or α-aminoadipic acid instead of glutamate showed ~40% and ~5%, respectively, of the L-glutamate activity. Moreover, enzymatic reactions including γ-glutamylglutamate, pyroglutamate, or *N*-acetyl-glutamate instead of L-glutamate showed no expected products.

Kinetic Study of MfnD. Because of the difficulties and complexities of global analysis of MfnD catalytic parameters, the apparent kinetic parameters of each substrate were obtained when MfnD was incubated with a fixed amount of the other two substrates. The apparent kinetic constants for tyramine followed Michaelis−Menten kinetics, and a $K_{M(tyramine)}$ = 0.80 mM and $k_{cat(app)}$ = 4.8 s^{-1} were obtained. A $K_{M(glutamate)}$ = 2.3 mM and

dx.doi.org/10.1021/bi500879h | *Biochemistry* 2014, 53, 6220−6230

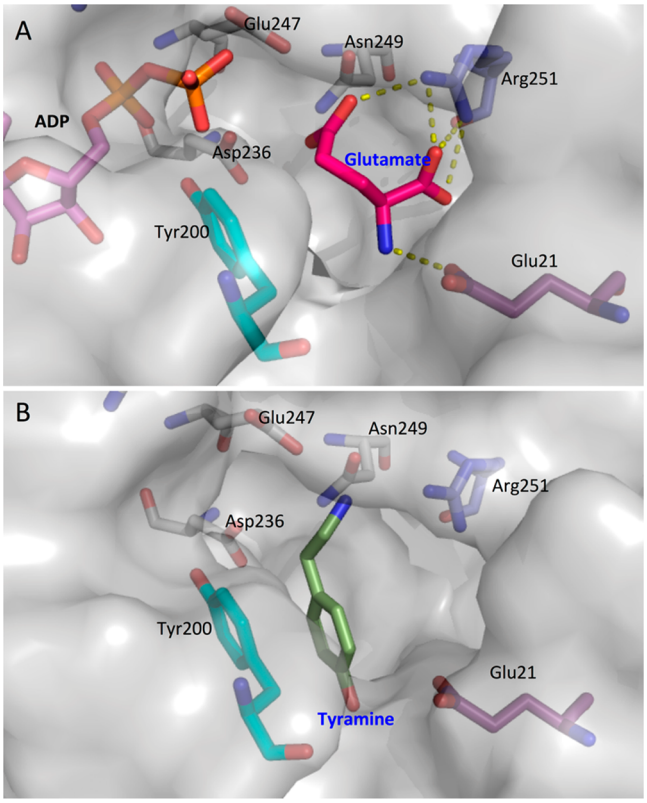

Figure 6. Molecular docking of L-glutamate (A) and tyramine (B) into the active site of MfnD. The L-glutamate and tyramine structures were obtained from the RCSB Protein Data Bank (PDB 4IWX and PDB 3BRA, respectively). The X-ray crystal structure of MfnD from *A. fulgidus* was deposited into the Protein Data Bank as PDB 3DF7. The ADP molecule shown in (A) is from the *E. coli* GS structure (PDB 1GSA) aligned with MfnD. Dotted lines indicate inferred polar contacts. Figure was generated and presented using MacPyMOL 1.3.[56]

$k_{cat(app)}$ = 5.8 s^{-1} were measured for the glutamate-dependent reaction. In terms of the ATP-dependent kinetic study, a $K_{M(ATP)}$ = 1.5 mM and a $k_{cat(app)}$ = 5.9 s^{-1} were obtained (Table 1). These catalytic parameters indicated that the catalytic ability of MfnD is comparable to other ATP-grasp enzymes, such as GS,[40] with a similar apparent k_{cat} and K_M.

Conserved Amino Acid Residues in MfnD. Despite structural similarities, the ATP-grasp superfamily overall exhibits low sequence identity.[18] However, multiple unique residues responsible for ATP-binding and metal binding are present in almost all the enzymes in this superfamily (Figure 4).[17] In MfnD and its homologues, Lys123 and Lys148 (numbers reflecting the gene product of Mefer_1180) corresponding to Lys125 and Lys160 in GS, likely interact with the α- and β-phosphate of ATP. Asp236, Glu247, and Asn249 corresponding to Asp273, Glu281, and Asn283 in GS participate in coordinating the metal ions.[23,24] In addition to these residues, Glu21, Ser176, Asn191, Gln193, Arg251, and Thr253 are strictly conserved in MfnD and its homologues (Figure 4). To identify the residues important for substrate binding and catalysis, we selectively generated three variants by site-directed mutagenesis. The steady-state parameters of these variants are listed in Table 1.

The Effect of Substitution of MfnD Conserved Residues on Enzymatic Activities. Single substitution of Glu21 or Thr253 caused a 3-fold decrease in $k_{cat(app)}$, and their apparent second-order constants k_{cat}/K_M were comparable to the wild-type, suggesting that their roles in the reaction mechanism were minor. In contrast, replacement of Arg251 with Ala caused a 100-fold decrease in $k_{cat(app)}$, indicating that it played an important role in catalysis. Notably, none of the substitutions caused a significant change in $K_{M(tyramine)}$ and $K_{M(ATP)}$. E21Q showed a slight increase in $K_{M(glutamate)}$, but R215A showed a more than 20-fold increase in $K_{M(glutamate)}$, suggesting that Arg251 was also responsible for glutamate binding.

The Crystal Structure of MfnD. The crystal structure of MfnD from *A. fulgidus* (the gene product of AF_1061, PDB 3DF7) was solved by Sugadev, R., et al. at New York SGX Research Center for Structural Genomics (AF_1061 shares 57% sequence similarity, 31% sequence identity with Mefer_1180). MfnD from *A. fulgidus* exists as a monomer. The overall structure exhibits a classical ATP-grasp fold with three structural domains[18] (Figure 5A) as seen in *E. coli* GS (Figure. 5B).[42] Because the residues responsible for ATP binding (Lys123 and Lys148) and the residues for metal binding (Asp236, Glu247, and Asn249) are conserved in the ATP grasp superfamily, it is reasonable to assume that ATP/ADP bind to a similar pocket in MfnD as seen from *E. coli* GS (Figure 5C,D). Although the residues involved in binding the adenine ring are not conserved, the adenine ring is likely buried in a similar hydrophobic pocket, stabilized by an aromatic amino acid (Figure 5C,D).

In the *E. coli* GS structure, Thr288 and Arg210 form hydrogen bonds with the C-terminal carboxyl group of the first substrate, γ-glutamylcysteine. The side chains of Ser286 and Thr288 are further involved in hydrogen bonding to the N-terminal nitrogen and carboxyl group of γ-glutamylcysteine, respectively (Figure 5D).[42] In the active site of MfnD, Glu21, Ser178, Arg251, Thr253, and Thr254 occupy the equivalent pocket, therefore, they might be important for glutamate binding. Of these, Glu21, Arg251, and Thr253 are strictly conserved in MfnD and its homologues (Figure. 4). The site-directed mutagenesis study showed that substitution of Glu21 or Thr253 only caused modest changes in the catalytic parameters. In contrast, replacement of Arg251 by Ala resulted in a significant decrease in $k_{cat(app)}$ and a more than 20-fold increase in $K_{M(glutamate)}$, indicating that it plays an important role in both catalysis and glutamate binding.

The Molecular Docking of L-Glutamate and Tyramine into MfnD. Molecular docking provides a possible binding position and orientation for each substrate at the active site. The docking model shown in Figure 6A shows that the γ-carboxylate of glutamate is in a position ready to accept a phosphate group from ATP to form an acyl phosphate intermediate. Arg251 likely anchors the glutamate by forming a hydrogen-bond network with the α- and γ-carboxylates of glutamate. In addition, the γ-carboxylate of Glu21 is within hydrogen bond distance of the α-amino group of the glutamate to further stabilize glutamate binding, consistent with the observation that the $K_{M(glutamate)}$ of E21Q was 3-fold higher than the wild-type. Although Arg251 and Glu21 are not present in most other ATP-grasp enzymes, a similar binding motif for L-glutamate is observed in glutamate cysteine ligase (GCL)[43,44] (not an ATP-grasp enzyme), which catalyzes the formation of γ-glutamylcysteine. In both cases, the γ-carboxylate of glutamate reacts with ATP to yield a reactive acyl phosphate intermediate, which then undergoes nucleophilic displacement by the amino group of the other substrate. The difficulty of such a mechanism is that free glutamyl-5-phosphate readily undergoes a cyclization reaction to form pyroglutamate (5-oxo-proline) and inorganic phosphate.[45,46] In GCL, Arg313 and Glu52 form hydrogen bonds with the α-carboxylate and α-amino group of the L-glutamate, respectively. Another Arg (Arg472) forms a polar contact with the γ-carboxylate of the L-

dx.doi.org/10.1021/bi500879h | *Biochemistry* 2014, 53, 6220−6230

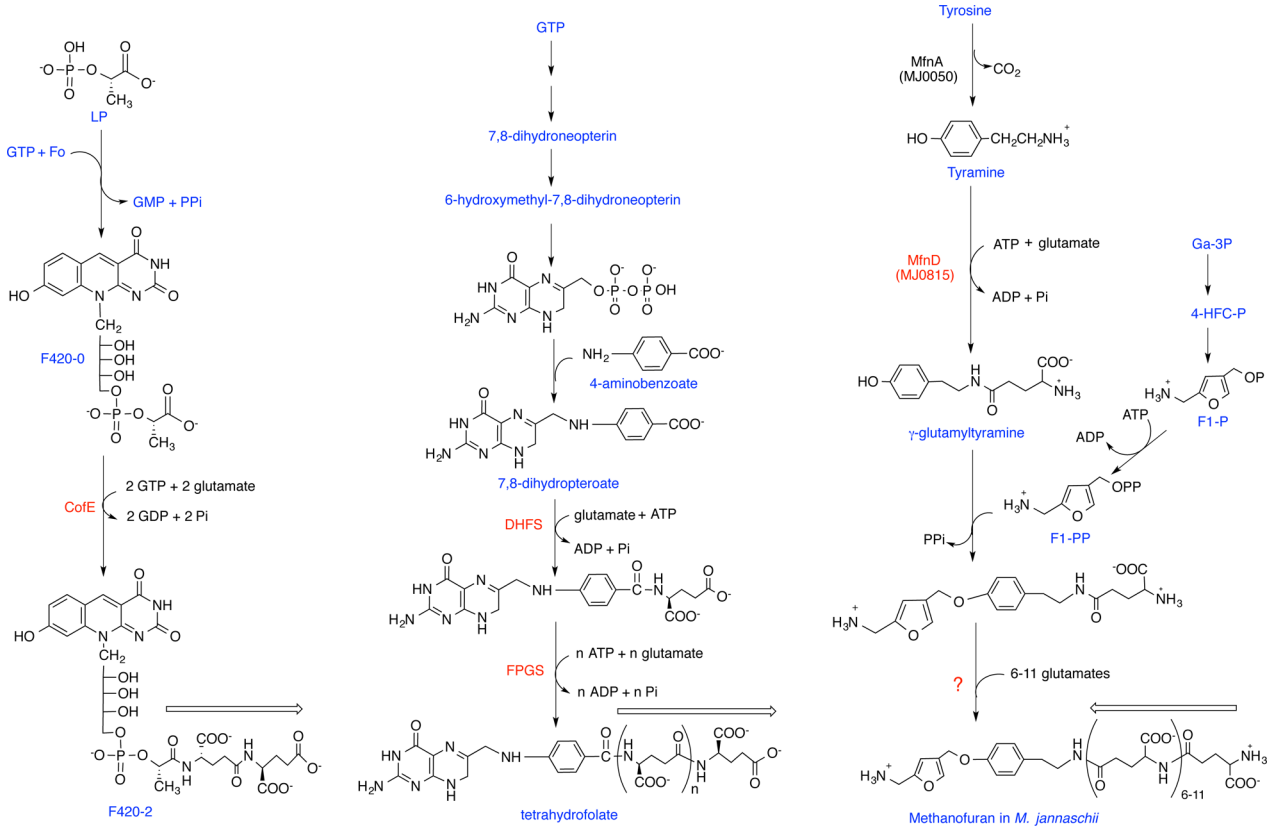

Figure 7. Comparison of the biosynthetic pathways of F_{420}, tetrahydrofolate, and methanofuran. Arrows indicate the γ-polyglutamate direction from amino terminus to carboxy terminus. Ga-3P, glyceraldehyde-3-P; F1-P, 5-(aminomethyl)-3-furanmethanol-phosphate; F1-PP, 5-(aminomethyl)-3-furanmethanol-pyrophosphate; 4-HFC-P, 4-(hydroxymethyl)-2-furancarboxaldehyde-phosphate; LP, 2-phospho-L-lactate; Fo, 7,8-didemethyl-8-hydroxy-5-deazaflavin; DHFS, dihydrofolate synthetase; FPGS, folypolyglutamate synthetase.

glutamate, stabilizing the γ-glutamyl phosphate intermediate.[43,47] In MfnD, only one Arg is conserved in the active site (Arg251). This residue appears to play important roles in both binding glutamate and stabilizing the labile intermediate, consistent with our site-directed mutagenesis results.

On the basis of the orientation of the glutathione molecule in GS, tyramine as an amino group donor likely appears at the same location as the glycine moiety in glutathione (Figure 5B), consistent with our docking result (Figure 6B). It shows that the aromatic ring of Tyr200 likely stabilizes the tyramine binding through stacking interactions; the amino group of tyramine is pointing toward the γ-carboxylate of glutamate (Figure 6B). Notably, the ATP-binding-induced conformational change is often observed in the ATP-grasp enzymes.[21,48,49] Therefore, the apo-MfnD structure (PDB 3DF7) might influence the docking accuracy.

Comparasion of F_{420}, Folate, and Methanofuran Biosynthesis. Poly γ-linked glutamate(s) are known to occur in the coenzymes of folate, F_{420}, and methanofuran (Figure 7). The number of γ-linked glutamate(s) in these cofactors varies among different organisms.[50−54] During F_{420} biosynthesis, CofE catalyzes the GTP-dependent addition of up to two γ-linked glutamates to F_{420}-0 to produce F_{420}-2 in *M. jannaschii*.[16] For the addition of the first glutamate, the amino group of the glutamate molecule forms the amide bond with the carboxylic acid group in F_{420}-0.[16] In the case of folate biosynthesis, two enzymes are required to catalyze the addition of glutamate residues. Dihydrofolate synthetase (DHFS) catalyzes the amide bond formation between the amino group of the first glutamate and the carboxylic acid group of dihydropteroate to produce dihydrofolate, after which folypolyglutamate synthetase (FPGS) catalyzes the polyglutamylation.[34,35] However, the direction of these amide bonds in methanofuran is reversed. MfnD catalyzes the amide bond formation between the amino group of tyramine and the γ-carboxyl group of the first glutamate (Figure 7). In addition, in both F_{420} and folate biosynthesis, the core component (F_{420}-0 and dihydropteroate, respectively) are synthesized first, followed by sequential addition of the required glutamate molecules. In contrast, in methanofuran biosynthesis, our results clearly show that γ-glutamyltyramine is synthesized first, and condensation with the furan moiety likely occurs later. We have recently found that the methanofuran in *M. jannaschii* contains 7−12 γ-linked glutamates.[57] Thus, the biosynthesis of methanofuran in *M. jannaschii* with 7−12 γ-linked glutamates is like folate biosynthesis, which requires two enzymes to add the γ-linked glutamates. In the case of methanofuran biosynthesis, MfnD catalyzes the addition of the first glutamate; another enzyme catalyzes the polyglutamylation to the molecule formed after the condensation of γ-glutamyltyramine with the furan moiety, producing the final methanofuran molecule (Figure 7). However, we have yet to identify the enzyme catalyzing this polyglutamylation.

CONCLUSION

This work describes a new enzyme catalyzing amide bond formation between the γ-carboxylate of glutamate and the amino group of tyramine. MJ0815/Mefer_1180, which encodes MfnD, is shown to be responsible for this reaction. In this study, we also

dx.doi.org/10.1021/bi500879h | *Biochemistry* 2014, 53, 6220−6230

describe the biochemical characterization of MfnD and the comparison of MfnD with *E. coli* GS on the basis of catalytic ability, structure, and catalytic residues. This study provides the first example of an ATP-grasp enzyme employing glutamate as the carboxylate substrate.

■ ASSOCIATED CONTENT

Supporting Information

Mass spectral analysis, data, and methods for analysis of tyramine in cell extracts, positive ion mode data from UPLC-ESI-HR-MS obtained from a cell extract of *M. jannaschii*, SDS-PAGE gels of MJ0815 and Mefer_1180, and MALDI-MS analysis of in-gel peptide data. This material is available free of charge via the Internet at http://pubs.acs.org.

■ AUTHOR INFORMATION

Corresponding Author

*Phone: (540) 231-6605. Fax: (540) 231-9070. E-mail: rhwhite@vt.edu.

Funding

This work was supported by National Science Foundation Grant MCB0722787.

Notes

The authors declare no competing financial interest.

■ ACKNOWLEDGMENTS

We thank Dr. Walter Niehaus, Dr. Suwen Zhao, and Dr. Kylie Allen for invaluable discussion and Dr. Janet Webster for editing the manuscript. We also thank Dr. W. Keith Ray for performing the mass spectrometry experiments. The mass spectrometry resources are maintained by the Virginia Tech Mass Spectrometry Incubator, a facility operated in part through funding by the Fralin Life Science Institute at Virginia Tech and by the Agricultural Experiment Station Hatch Program (CRIS project no.: VA-135981).

■ ABBREVIATIONS USED

GS, glutathione synthetase; DHFS, dihydrofolate synthetase; FPGS, folypolyglutamate synthetase; 4-HFC-P, 4-(hydroxymethyl)-2-furancarboxaldehyde-P; Ga-3P, glyceraldehyde-3-P; F1-P, 5-(aminomethyl)-3-furanmethanolphosphate; F1-PP, 5-(aminomethyl)-3-furanmethanolpyrophosphate; γ-glutamyltyramine, 2-amino-5-((4-hydroxyphenethyl) amino)-5-oxopentanoic acid; THF, tetrahydrofuran; DCC, dicyclohexylcarbodiimide solution; APMF, 4-[[4-(2-aminoethyl)phenoxy]-methyl]-2-furanmethanamine; APMF-$(Glu)_2$, 4-[*N*-(γ-L-glutamyl-γ-L-glutamyl)-*p*-(β-aminoethyl)phenoxymethyl]-2-(aminomethyl)-furan; fural-tyramine, 2-(4-(furan-3-ylmethoxy)phenyl)ethan-1-amine; TCA, trichloroacetic acid; Tricine, *N*-(2-hydroxy-1,1-bis(hydroxymethyl)ethyl)glycine; CAPS, 3-(cyclohexylamino)-1-propanesulfonic acid; TES, 2-[[1,3-dihydroxy-2-(hydroxymethyl)propanyl]-2-amino]ethanesulfonic acid; EDTA, ethylenediaminetetraacetic acid

■ ADDITIONAL NOTE

[a]Since the publication of ref 7, we found new evidence that 4-HFC-P syntase (MfnB) employs Ga-3P as the sole substrate.

■ REFERENCES

(1) Ferry, J. G. (1999) Enzymology of one-carbon metabolism in methanogenic pathways. *FEMS Microbiol. Rev. 23*, 13−38.

(2) Deppenmeier, U. (2002) The unique biochemistry of methanogenesis. *Prog. Nucleic Acid Res. Mol. Biol. 71*, 223−283.

(3) Leigh, J. A., Rinehart, K. L., and Wolfe, R. S. (1984) Structure of Methanofuran, the Carbon-Dioxide Reduction Factor of *Methanobacterium thermoautotrophicum*. *J. Am. Chem. Soc. 106*, 3636−3640.

(4) Chistoserdova, L., Vorholt, J. A., Thauer, R. K., and Lidstrom, M. E. (1998) C1 transfer enzymes and coenzymes linking methylotrophic bacteria and methanogenic Archaea. *Science 281*, 99−102.

(5) Pomper, B. K., and Vorholt, J. A. (2001) Characterization of the formyltransferase from *Methylobacterium extorquens* AM1. *Eur. J. Biochem. 268*, 4769−4775.

(6) White, R. H. (1988) Structural Diversity among Methanofurans from Different Methanogenic Bacteria. *J. Bacteriol. 170*, 4594−4597.

(7) Miller, D., Wang, Y., Xu, H., Harich, K., and White, R. H. (2014) Biosynthesis of the 5-(Aminomethyl)-3-furanmethanol Moiety of Methanofuran. *Biochemistry 53*, 4635−4647.

(8) Kezmarsky, N. D., Xu, H., Graham, D. E., and White, R. H. (2005) Identification and characterization of a L-tyrosine decarboxylase in *Methanocaldococcus jannaschii*. *Biochim. Biophys. Acta 1722*, 175−182.

(9) von Dohren, H., Keller, U., Vater, J., and Zocher, R. (1997) Multifunctional Peptide Synthetases. *Chem. Rev. 97*, 2675−2706.

(10) Marahiel, M. A., Stachelhaus, T., and Mootz, H. D. (1997) Modular Peptide Synthetases Involved in Nonribosomal Peptide Synthesis. *Chem. Rev. 97*, 2651−2674.

(11) Cane, D. E., Walsh, C. T., and Khosla, C. (1998) Harnessing the biosynthetic code: combinations, permutations, and mutations. *Science 282*, 63−68.

(12) Donadio, S., Staver, M. J., McAlpine, J. B., Swanson, S. J., and Katz, L. (1991) Modular organization of genes required for complex polyketide biosynthesis. *Science 252*, 675−679.

(13) Iyer, L. M., Abhiman, S., Maxwell Burroughs, A., and Aravind, L. (2009) Amidoligases with ATP-grasp, glutamine synthetase-like and acetyltransferase-like domains: synthesis of novel metabolites and peptide modifications of proteins. *Molecular BioSyst. 5*, 1636−1660.

(14) Graham, D. E., and White, R. H. (2002) Elucidation of methanogenic coenzyme biosynthesis: from spectroscopy to genomics. *Nat. Prod. Rep. 19*, 133−147.

(15) Kleinkauf, H., and Von Dohren, H. (1996) A nonribosomal system of peptide biosynthesis. *Eur. J. Biochem. 236*, 335−351.

(16) Li, H., Graupner, M., Xu, H., and White, R. H. (2003) CofE catalyzes the addition of two glutamates to F_{420}-0 in F_{420} coenzyme biosynthesis in *Methanococcus jannaschii*. *Biochemistry 42*, 9771−9778.

(17) Galperin, M. Y., and Koonin, E. V. (1997) A diverse superfamily of enzymes with ATP-dependent carboxylate-amine/thiol ligase activity. *Protein Sci. 6*, 2639−2643.

(18) Fawaz, M. V., Topper, M. E., and Firestine, S. M. (2011) The ATP-grasp enzymes. *Bioorg. Chem. 39*, 185−191.

(19) Artymiuk, P. J., Poirrette, A. R., Rice, D. W., and Willett, P. (1996) Biotin carboxylase comes into the fold. *Nature Struct. Biol. 3*, 128−132.

(20) Fan, C., Moews, P. C., Shi, Y., Walsh, C. T., and Knox, J. R. (1995) A common fold for peptide synthetases cleaving ATP to ADP: glutathione synthetase and D-alanine:D-alanine ligase of *Escherichia coli*. *Proc. Natl. Acad. Sci. U. S. A. 92*, 1172−1176.

(21) Thoden, J. B., Firestine, S., Nixon, A., Benkovic, S. J., and Holden, H. M. (2000) Molecular structure of *Escherichia coli* PurT-encoded glycinamide ribonucleotide transformylase. *Biochemistry 39*, 8791−8802.

(22) Wang, W., Kappock, T. J., Stubbe, J., and Ealick, S. E. (1998) X-ray crystal structure of glycinamide ribonucleotide synthetase from *Escherichia coli*. *Biochemistry 37*, 15647−15662.

(23) Griffith, O. W., and Mulcahy, R. T. (1999) The enzymes of glutathione synthesis: gamma-glutamylcysteine synthetase. *Adv. Enzymol. Relat. Areas Mol. Biol. 73*, 209−267 xii..

(24) Hibi, T., Nii, H., Nakatsu, T., Kimura, A., Kato, H., Hiratake, J., and Oda, J. (2004) Crystal structure of gamma-glutamylcysteine synthetase: insights into the mechanism of catalysis by a key enzyme for glutathione homeostasis. *Proc. Natl. Acad. Sci. U. S. A. 101*, 15052−15057.

(25) Makarova, K. S., Aravind, L., Galperin, M. Y., Grishin, N. V., Tatusov, R. L., Wolf, Y. I., and Koonin, E. V. (1999) Comparative genomics of the Archaea (Euryarchaeota): evolution of conserved protein families, the stable core, and the variable shell. *Genome Res. 9*, 608−628.
(26) Li, H., Xu, H., Graham, D. E., and White, R. H. (2003) Glutathione synthetase homologs encode alpha-L-glutamate ligases for methanogenic coenzyme F_{420} and tetrahydrosarcinapterin biosyntheses. *Proc. Natl. Acad. Sci. U. S. A. 100*, 9785−9790.
(27) Kalyuzhnaya, M. G., Korotkova, N., Crowther, G., Marx, C. J., Lidstrom, M. E., and Chistoserdova, L. (2005) Analysis of gene islands involved in methanopterin-linked C1 transfer reactions reveals new functions and provides evolutionary insights. *J. Bacteriol. 187*, 4607−4614.
(28) Chistoserdova, L., Chen, S. W., Lapidus, A., and Lidstrom, M. E. (2003) Methylotrophy in *Methylobacterium extorquens* AM1 from a genomic point of view. *Jou. Bacteriol. 185*, 2980−2987.
(29) White, R. H., and Xu, H. (2006) Methylglyoxal Is an Intermediate in the Biosynthesis of 6-Deoxy-5-ketofructose-1-phosphate: A Precursor for Aromatic Amino Acid Biosynthesis in *Methanocaldococcus jannaschii*. *Biochemistry 45*, 12366−12379.
(30) Bradford, M. M. (1976) A rapid and sensitive method for the quantitation of microgram quantities of protein utilizing the principle of protein−dye binding. *Anal. Biochem. 72*, 248−254.
(31) Morris, G. M., H, R., Lindstrom, W., Sanner, M. F., Belew, R. K., Goodsell, D. S., and Olson, A. J. (2009) AutoDock 4 and AutoDock Tools 4: automated docking with selective receptor flexibility. *J. Comput. Chem. 16*, 2785−2791.
(32) Trott, O., and Olson, A. J. (2010) AutoDock Vina: Improving the Speed and Accuracy of Docking with a New Scoring Function, Efficient Optimization, and Multithreading. *J. Comput. Chem. 31*, 455−461.
(33) Pettersen, E. F., Goddard, T. D., Huang, C. C., Couch, G. S., Greenblatt, D. M., Meng, E. C., and Ferrin, T. E. (2004) UCSF Chimera—a visualization system for exploratory research and analysis. *J. Comput. Chem. 25*, 1605−1612.
(34) Bermingham, A., and Derrick, J. P. (2002) The folic acid biosynthesis pathway in bacteria: evaluation of potential for antibacterial drug discovery. *Bioessays 24*, 637−648.
(35) Hanson, A. D., and Gregory, J. F., III. (2011) Folate biosynthesis, turnover, and transport in plants. *Annu. Rev. Plant Biol. 62*, 105−125.
(36) Esser, L., Wang, C. R., Hosaka, M., Smagula, C. S., Sudhof, T. C., and Deisenhofer, J. (1998) Synapsin I is structurally similar to ATP-utilizing enzymes. *EMBO J. 17*, 977−984.
(37) Gitler, D., Xu, Y., Kao, H. T., Lin, D., Lim, S., Feng, J., Greengard, P., and Augustine, G. J. (2004) Molecular determinants of synapsin targeting to presynaptic terminals. *J. Neurosci. 24*, 3711−3720.
(38) Kyte, J. (1995) *Mechanism in Protein Chemistry*, pp 355−356, Garland Publishing, New York and London.
(39) Sigel, H. (1987) Isomeric equilibria in complexes of adenosine 5′-triphosphate with divalent metal ions. Solution structures of M(ATP)2-complexes. *Eur. J. Biochem./FEBS 165*, 65−72.
(40) Gushima, H., Miya, T., Murata, K., and Kimura, A. (1983) Purification and characterization of glutathione synthetase from *Escherichia coli B*. *J. Appl. Biochem 5*, 210−218.
(41) Ownby, K., Xu, H., and White, R. (2005) A *Methanocaldococcus jannaschii* archeal signature gene encodes for a 5-formaminoimidazole-4-carboxamide-1-β-D-ribofuranosyl 5′-monophosphate synthetase: a new enzyme in purine biosynthesis. *J. Biol. Chem. 280*, 10881−10887.
(42) Hara, T., Kato, H., Katsube, Y., and Oda, J. (1996) A pseudo-Michaelis quaternary complex in the reverse reaction of a ligase: structure of *Escherichia coli B* glutathione synthetase complexed with ADP, glutathione, and sulfate at 2.0 A resolution. *Biochemistry 35*, 11967−11974.
(43) Biterova, E. I., and Barycki, J. J. (2009) Mechanistic details of glutathione biosynthesis revealed by crystal structures of *Saccharomyces cerevisiae* glutamate cysteine ligase. *J. Biol. Chem. 284*, 32700−32708.
(44) Galant, A., Arkus, K. A., Zubieta, C., Cahoon, R. E., and Jez, J. M. (2009) Structural basis for evolution of product diversity in soybean glutathione biosynthesis. *Plant Cell 21*, 3450−3458.
(45) Seddon, A. P., Zhao, K. Y., and Meister, A. (1989) Activation of glutamate by gamma-glutamate kinase: formation of gamma-*cis*-cycloglutamyl phosphate, an analog of gamma-glutamyl phosphate. *J. Biol. Chem. 264*, 11326−11335.
(46) Hayzer, D. J., and Moses, V. (1978) The enzymes of proline biosynthesis in *Escherichia coli*. Their molecular weights and the problem of enzyme aggregation. *Biochem. J. 173*, 219−228.
(47) Abbott, J. J., Ford, J. L., and Phillips, M. A. (2002) Substrate binding determinants of *Trypanosoma brucei* gamma-glutamylcysteine synthetase. *Biochemistry 41*, 2741−2750.
(48) Sloane, V., Blanchard, C. Z., Guillot, F., and Waldrop, G. L. (2001) Site-directed mutagenesis of ATP binding residues of biotin carboxylase. Insight into the mechanism of catalysis. *J. Biol. Chem. 276*, 24991−24996.
(49) Zhang, Y., White, R. H., and Ealick, S. E. (2008) Crystal structure and function of 5-formaminoimidazole-4-carboxamide ribonucleotide synthetase from *Methanocaldococcus jannaschii*. *Biochemistry 47*, 205−217.
(50) Bair, T. B., Isabelle, D. W., and Daniels, L. (2001) Structures of coenzyme F_{420} in *Mycobacterium* species. *Arch. Microbiol. 176*, 37−43.
(51) Isabelle, D., Simpson, D. R., and Daniels, L. (2002) Large-scale production of coenzyme F_{420}-5,6 by using *Mycobacterium smegmatis*. *Appl. Environ. Microbiol. 68*, 5750−5755.
(52) Forouhar, F., Abashidze, M., Xu, H., Grochowski, L. L., Seetharaman, J., Hussain, M., Kuzin, A., Chen, Y., Zhou, W., Xiao, R., Acton, T. B., Montelione, G. T., Galinier, A., White, R. H., and Tong, L. (2008) Molecular insights into the biosynthesis of the F_{420} coenzyme. *J. Biol. Chem. 283*, 11832−11840.
(53) Osborne, C. B., Lowe, K. E., and Shane, B. (1993) Regulation of folate and one-carbon metabolism in mammalian cells. I. Folate metabolism in Chinese hamster ovary cells expressing *Escherichia coli* or human folylpoly-gamma-glutamate synthetase activity. *J. Biol. Chem. 268*, 21657−21664.
(54) Toy, J., and Bognar, A. L. (1994) Mutagenesis of the *Lactobacillus casei* folylpolyglutamate synthetase gene at essential residues resembling an ATP binding site. *Arch. Biochem. Biophys. 314*, 344−350.
(55) Gille, C., Fahling, M., Weyand, B., Wieland, T., and Gille, A. (2014) Alignment-Annotator web server: rendering and annotating sequence alignments. *Nucleic Acids Res. 42*, W3−6.
(56) DeLano, W. L. (2009) PyMOL molecular viewer: updates and refinements, *Abstracts of Papers of the American Chemical Society*, Washington, DC, Vol. *238*.
(57) Allen, K. D., and White, R. H. (2014) Identification of structurally diverse methanofuran coenzymes in Methanococcales that are both N-formylated and N-acetylatedIdentification of structurally diverse methanofuran coenzymes in Methanococcales that are both N-formylated and N-acetylated. *Biochemistry*, DOI: 10.1021/bi500973h.